





Article

Adsorption of Cobalt and Strontium Ions on Plant-Derived Activated Carbons: The Suggested Mechanisms

Irina Ceban (Ginsari)¹, Tudor Lupascu¹, Sergey Mikhailovsky^{2,3} and Raisa Nastas^{1,*}

¹ Institute of Chemistry, Moldova State University, 3, Academiei Str., 2028 Chisinau, Moldova; irina.ginsari@ichem.md (I.C.); lupascut@gmail.com (T.L.)

² ANAMAD Ltd., Sussex Innovation Centre, Science Park Square, Falmer, Brighton BN1 9SB, UK; sergeymikhailovsky@gmail.com

³ Chuiko Institute of Surface Chemistry, National Academy of Sciences of Ukraine 17, General Naumov Str., 03164 Kyiv, Ukraine

* Correspondence: raisa.nastas@ichem.md

Abstract: In this study, activated carbons derived from walnut shells (CA-N) and apple wood (CA-M) were used as adsorbents to remove cobalt(II) and strontium(II) ions from aqueous solutions. The novel materials were obtained using nitric acid (CA-Mox) and nitric acid/urea mixture (CA-Mox-u, CA-Nox-u) as oxidizing agents. The physical–chemical characteristics of activated carbons were determined from nitrogen sorption isotherms, SEM-EDX, FTIR, pH metric titrations, the Boehm titration method and elemental analysis. The results of batch experiments indicate that maximum adsorption can be achieved in broad pH ranges: 4–8 for Co(II) and 4–10 for Sr(II). The maximum adsorption capacities of Co(II) and Sr(II) on oxidized activated carbons at pH = 4 are: CA-Mox, 0.085 and 0.076 mmol/g; CA-Mox-u, 0.056 and 0.041 mmol/g; and CA-Nox-u, 0.041 and 0.034 mmol/g, respectively. The mathematical models (pseudo-first-order, pseudo-second-order and intraparticle diffusion kinetic models, and Langmuir, Freundlich, Dubinin–Radushkevich, and Temkin–Pyzhev isotherm models) were used to explain the adsorption kinetics, to study the adsorption mechanism and predict maximum adsorption capacity of the adsorbents. The adsorption mechanisms of toxic metal ions on activated carbons were proposed.

Keywords: activated carbons; modification; adsorption; cobalt ions; strontium ions



Citation: Ceban, I.; Lupascu, T.; Mikhailovsky, S.; Nastas, R. Adsorption of Cobalt and Strontium Ions on Plant-Derived Activated Carbons: The Suggested Mechanisms. *C* **2023**, *9*, 71. <https://doi.org/10.3390/c9030071>

Academic Editor: Jorge Bedia

Received: 5 June 2023

Revised: 3 July 2023

Accepted: 10 July 2023

Published: 21 July 2023



Copyright: © 2023 by the authors. Licensee MDPI, Basel, Switzerland. This article is an open access article distributed under the terms and conditions of the Creative Commons Attribution (CC BY) license (<https://creativecommons.org/licenses/by/4.0/>).

1. Introduction

Several studies have confirmed that heavy metals are toxic to different life forms (e.g., plants, aquatic organisms and humans) and can generate a significant environmental impact. With the increase in the number of nuclear reactors, radioactive pollution of water and soil is increasing. Heavy and radioactive metals (such as lead, cadmium, arsenic, cesium, strontium, cobalt, mercury, chromium, etc.) are persistent pollutants with potential hazards, which have high toxicity, are nonbiodegradable and easily accumulate in organisms from food and/or drinking water [1–6]. Several acute and chronic toxic effects of heavy metals affect different body organs. Gastrointestinal and kidney dysfunction, nervous system disorders, skin lesions, vascular damage, immune system dysfunction, birth defects and cancer are examples of the complications of heavy metals toxic effects [1,5,6]. Radioactive heavy metals have a more complex effect on the living organism, as the ionizing radiation of the incorporated ions can break down DNA, proteins and other biomolecules [7,8]. Adsorption on activated carbons is one of the often-used procedures to remove toxic metals from fluids [9–18]. This separation process implies the transfer of metal ions from the fluid (i.e., water or industrial effluent) to the surface of a solid matrix (i.e., adsorbent) that should have a tailored surface chemistry and porosity to reach an effective separation. The effectiveness of the adsorption of heavy metal ions is affected by several operating variables like contact time, adsorbent amount, temperature, initial metal concentration and

pH [11–13,18]. Also, textural parameters and surface chemistry of the activated carbon are essential to achieve the successful removal of toxic metals.

Activated carbons from plant-derived raw (agro-based) materials are low-cost adsorbents and are considered in agricultural countries with large amounts of agricultural waste produced every year. Among the plant-derived materials used to obtain activated carbons are nut shells, grape seeds, plum stones, peach stones, tree wood, rice husk, sawdust, wheat straw, etc. [3,4,12–14,16–19]. As was mentioned above, among the important activated carbons characteristics that influence the adsorption of metals is surface chemistry. In the literature, several types of surface tailoring and modification of activated carbons were reported, including nitric acid, peroxide and ozone oxidation, sulphuration and nitrogenating treatment, as well as anchoring coordination ligands [13,14,16,20].

In the current work, nitric acid was selected as an oxidation agent for the modification of activated carbon surface chemistry. In addition to the traditional method, a modified method was also applied, using as an oxidizing agent the mixture of nitric acid and urea. The indirect role of urea is to protect the activated carbon surface from excessive degradation with the formation of humic acids [21].

Preliminary results of adsorption of toxic metal ions (such as lead, mercury, cobalt, cadmium, strontium and caesium) from solution on walnut shells (CA-N) and apple wood (CA-M)-activated carbons highlight samples modified by oxidation, and cobalt, lead, cadmium and strontium ions are best adsorbed [22].

The present study aimed to investigate the adsorption behavior of Co(II) and Sr(II) ions on the surface of plant-derived activated carbons (obtained from walnut shells and apple wood, and modified by oxidation with nitric acid and nitric acid/urea mixture). The pseudo-first-order, pseudo-second-order and intraparticle diffusion models were used to explain the adsorption kinetics and accessibility of the heavy metal ions, while Langmuir, Freundlich, Dubinin–Radushkevich, and Temkin–Pyzhev isotherm models were used to study the adsorption mechanism and predict maximum adsorption capacity of the adsorbents. By summarizing the obtained results, the adsorption mechanisms of toxic metal ions on activated carbons were proposed.

2. Materials and Methods

Cobalt nitrate ($\text{Co}(\text{NO}_3)_2 \cdot 6\text{H}_2\text{O}$), strontium nitrate ($\text{Sr}(\text{NO}_3)_2$), nitric acid (HNO_3), hydrochloric acid (HCl), sodium hydroxide (NaOH) and urea (NH_2CONH_2) were purchased from Sigma-Aldrich Chemie GmbH (Taufkirchen, Germany). All used reagents were of analytical grade and were used without additional purification. Water used for solution preparations was distilled twice.

2.1. Modification and Characterization of Activated Carbons

In this research, carbonaceous adsorbents of local origin were used; activated carbons obtained from walnuts shells (CA-N) and apple wood (CA-M) by physical–chemical activation method with water steam were provided by LLC Ecosorbent (Republic of Moldova).

- Modification of activated carbons surface by oxidation with nitric acid

The oxidation process of activated carbons by the classical method was carried out as follows [13,23,24]: concentrated nitric acid solution (63%) was added to 500 g of granular activated carbon CA-M, fraction $0.63 \div 0.8$ mm (at a solid (g):liquid (mL) ratio of 1:3), which was placed in a glass flask on the water bath (the scheme installation is presented in Appendix S1). The mixture of nitric acid and activated carbon was kept at 95°C for 8 h. The released nitrogen oxides (off-gases) were collected in the collection vessel filled with sodium hydroxide solution. After the oxidation process was finished, the mixture was cooled and decanted. Humic and fulvic acids formed during the oxidation process were removed with a 1.0 N potassium hydroxide solution, and then by repeated washing with distilled water until the washing solution color changed from brown to yellow. After removing the humic acids, the oxidized activated carbon was converted to the H^+ form by treatment with a 1.0 N solution of hydrochloric acid. Afterward, the oxidized activated

carbon was washed with distilled water until the negative reaction of chlorine ions, then dried at 110 ± 5 °C and labeled as CA-Mox.

- *Modification of activated carbons surface by oxidation with nitric acid/urea mixture*

The oxidation with nitric acid/urea mixture was carried out as follows: activated carbon (500 g) (CA-N or CA-M) was introduced into the flask to which the mixture of nitric acid and urea in a molar ratio of 3:1 was added (at a solid (g):liquid (mL) ratio of 1:3) (Appendix S1). The oxidation process took about 10–12 h at a temperature of 95 °C. The released gases were collected in the collection vessel filled with sodium hydroxide solution. After the oxidation process was finished, the mixture was cooled and decanted. The formation of humic and fulvic acids was checked with a 1.0 N potassium hydroxide solution and, since the respective acids were not formed, the steps of washing the oxidized activated carbon with the basic solution and its conversion into H form were omitted. The oxidized activated carbons were washed with distilled water until the negative reaction of nitrate/nitrite ions, then dried at 110 ± 5 °C and labeled as CA-Mox-u, CA-Nox-u.

During the oxidation of activated carbon with nitric acid, the presence of urea is necessary, which, acts as a buffer (nitric acid in combination with urea forms a soluble complex $\text{H}_2\text{NCONH}_2 \cdot \text{HNO}_3$ that reduces the oxidation capacity of nitric acid), protecting the activated carbon by absorbing nitrogen oxides released during oxidation, thus preventing the formation of humic compounds [13,21,24,25] (a detailed explanation is presented in Appendix S2).

For the experiments, an activated carbons grain fraction of $0.63 \div 0.8$ mm was selected. Prior to all experiments activated carbons samples were dried in an oven at 110 ± 5 °C for at least 3 h.

- *Characterization of activated carbons*

The physical–chemical characteristics of activated carbons were evaluated by general indices (ash A, humidity U, and elemental analysis). Humidity and ash content in activated carbons were determined by standard methods [26]. The elemental analysis (C, H, N, S) was determined on the Elemental analyzer CHNS Vario EL III (Elementar Analysensysteme GmbH, Langenselbold, Germany). SEM-EDX profiles of the samples were obtained by the Scanning Electron Microscope (SEM), model VEGA II LSH (TESCAN Co., Libušina, Czech Republic) coupled with Energy Dispersive X-ray detector (EDX), type QUANTAX QX2 (BRUKER/ROENTEC Co., Berlin, Germany).

Porous structure characteristics of active carbons were determined from sorption isotherms of nitrogen at 77 K measured using Autosorb-1MP (Quantachrome Instruments, Boynton Beach, FL, USA). The specific surface area (S_{BET}) was calculated using the Brunauer–Emmett–Teller (BET) equation. The total pore volume (V_{total}) was calculated by converting the amount of nitrogen gas adsorbed at a relative pressure of 0.99 to the equivalent liquid volume of the adsorbate. The volume of micropores (V_{micro}) was determined using the *t*-method, and the volume of mesopores (V_{meso}) was determined from the difference between the total volume and the volume of micropores.

The surface chemistry of the activated carbons has been evaluated by jointing infrared spectroscopy (FTIR), pH metric titrations and the Boehm titration method. The IR spectra of activated carbons were recorded by FT-IR Spectrum 100 apparatus (PerkinElmer, Shelton, CT, USA), using dilutions in potassium bromide. The Boehm titration method (proposed by H.P. Boehm in 1966 [27,28]) is based on the theory that acid and base in an aqueous solution react with different basic and acidic functional groups on the surface of activated carbons which are derived from different oxygenated functional groups [13,27,28]. Experimental details are presented in the literature [27–29] (Appendix S3). The results of pH metric titrations were used to determine pH_{pzc} and acidity constants of surface groups of activated carbons [29,30]. The activated carbon pH_{pzc} was determined from the intersection of proton-binding isotherms obtained for three concentrations of background electrolyte (0.1 M, 0.05 M and 0.01 M NaCl) [29] (Appendix S4). Proton affinity distributions, $F(\text{pKa})$,

were calculated from proton-binding isotherms by solving the adsorption integral equation using the CONTIN method [31–34].

- *Determination of metals*

Determination of cobalt(II) and strontium(II) ions, as well as metals on activated carbons ash, was performed on AAS-1N (Carl Zeiss, Industrielle Messtechnik GmbH, Oberkochen, Germany) and Shimadzu AA7000 (Shimadzu Co., Kyoto, Japan) atomic absorption spectrometers, respectively, depending on metals concentration in solution.

- *Determination of metals species in solution as pH*

The cobalt and strontium speciation in the solution was calculated/estimated by Visual MINTEQ software, version 4.0 (4.04) [35].

2.2. Adsorption Experiments

The metals salts ($\text{Co}(\text{NO}_3)_2$, $\text{Sr}(\text{NO}_3)_2$) solutions ($0.2\text{--}2\text{ mmolL}^{-1}$) were added to 0.05 g of adsorbent dosage, at a solid (g):liquid (mL) ratio of 1:100. The mixtures of adsorbent–adsorbate were agitated in a shaker, between 10 and 600 min, at a temperature of $20 \pm 2\text{ }^\circ\text{C}$. The samples were filtered to separate the adsorbent from the metal solution. The concentration of metal ions in the solution was determined by AAS at a wavelength of 240.7 nm for cobalt(II) and 460 nm for strontium(II). The pH of the solutions was adjusted using HNO_3 and NaOH solutions.

The capacity (a , mmol g^{-1}) of adsorption and removal efficiency (R , %) were calculated using Equations (1) and (2), respectively.

$$a = \frac{(C_0 - C_e) \cdot V}{m} \quad (1)$$

$$R = \frac{(C_0 - C_e) \cdot 100}{C_0} \quad (2)$$

where C_0 is the initial concentration (mmolL^{-1}); and C_e is the equilibrium concentration (mmolL^{-1}); m is mass of adsorbent; and V the volume of solution (L).

The pseudo-first-order (Lagergren) [36], pseudo-second-order (Ho and McKay) [37] and intraparticle diffusion (Weber–Morris) [38,39] models were used to analyze the kinetic data. The linearized expressions of the theoretical models are shown in Equations (3)–(5), respectively.

$$\ln(q_e - q_t) = \ln(q_e) - k_1 t \quad (3)$$

$$\frac{t}{q_t} = \frac{t}{q_e} + \frac{1}{k_2 q_e^2} \quad (4)$$

$$q_t = k_i t^{1/2} \quad (5)$$

where q_e and q_t is the adsorption capacity (mmol/g) at equilibrium and time t (min); k_1 is the pseudo-first-order constant (min^{-1}); k_2 is the pseudo-second-order constant ($\text{mmol g}^{-1} \text{min}^{-1}$); and k_i is the intraparticle constant ($\text{mmol/g min}^{1/2}$).

The adsorption isotherms data were fitted to the mathematical models Langmuir [40], Freundlich [41], Dubinin–Radushkevich [42] and Temkin–Pyzhev [43], as presented in Equations (6)–(9). The essential characteristics of Langmuir isotherm are expressed in terms of a dimensionless constant separation factor R_L (equilibrium parameters) that is given in Equation (10).

$$q_e = \frac{Q_0 K_L C_e}{1 + K_L C_e} \quad (6)$$

$$q_e = K_F C_e^{1/n} \quad (7)$$

$$q_e = (q_s) \exp - k_{ads} \varepsilon^2 \quad (8)$$

$$q_e = \left(\frac{RT}{b} \right) \ln(K_T C_e) \quad (9)$$

$$R_L = \frac{1}{1 + K_L C_0} \quad (10)$$

where q_e is the adsorption capacity (mmol/g) at equilibrium; Q_0 is the monolayer capacity (mmol/g); K_L is the Langmuir adsorption constant (L/mmol); K_F is the Freundlich equilibrium constant; q_s is the saturation capacity (mmol/g); K_{ads} and ε are the constants of the Dubinin–Radushkevich isotherm; K_T is the constant of Temkin–Pyzhev model; n is the parameter characterizing the system heterogeneity.

3. Results and Discussion

3.1. Characterization of the Activated Carbons

The modification of activated carbons via oxidation with concentrated nitric acid (CA-Mox sample) and with nitric acid/urea mixture (CA-Mox-u and CA-Nox-u samples) leads to a decrease in ash content from ~3% to ~0.6% (Table 1). The content of metals determined via AAS, and completed by the SEM-EDX results, reveals that after the oxidation process, traces of metals remain, while all the manganese, sodium and iron compounds are mostly removed (Table S1, Figure S1).

Table 1. The general characteristics of activated carbons.

Sample	U *, %	A **, %	Elemental Analysis, %			
			C	H	N	S
CA-N	13.11 ± 0.44	2.94 ± 0.23	92.52	1.24	0.07	0
CA-M	8.65 ± 0.03	1.06 ± 0.04	92.00	1.38	0.26	0
CA-Nox-u	14.76 ± 0.23	0.95 ± 0.06	88.43	1.42	0.85	0
CA-Mox-u	15.49 ± 0.41	0.87 ± 0.12	81.81	1.80	1.05	0
CA-Mox	5.26 ± 0.40	0.56 ± 0.11	81.73	1.60	0.69	0

* U—humidity. ** A—ash content.

The porous structure characteristics of the samples determined from the nitrogen sorption–desorption isotherms are presented in Table 2. The results show that after the oxidation process, either for activated carbon obtained from nut shells (CA-N), as well as, for activated carbon obtained from apple wood (CA-M), there is a decrease in the values of S_{BET} of the carbonaceous adsorbents, V_{total} and V_{meso} , whereas V_{micro} is almost unchanged (Table 2). The decrease in V_{total} is mainly due to V_{meso} , and this can be explained by the formation of functional groups on the surface of mesopores in the process of oxidation of the activated carbon. Functional groups cannot form in the micropores because of their length compared to the size of the micropores. According to data from the literature, there is a decrease in S_{BET} and V_{total} after the oxidation process, which in certain cases is explained by the formation of functional groups and pores being blocked [13].

Table 2. Porous structure characteristics of activated carbons, determined from N₂ sorption isotherms.

Sample	S_{BET} , m ² /g	V_{total} , cm ³ /g	V_{micro} , cm ³ /g	V_{meso} , cm ³ /g
CA-M	812	0.540	0.240	0.300
CA-N	782	0.505	0.235	0.270
CA-Mox	670	0.361	0.225	0.136
CA-Mox-u	719	0.416	0.233	0.183
CA-Nox-u	696	0.411	0.230	0.181

The presence of functional groups on the surface of activated carbons obtained from walnut shells and apple wood has been determined by IR spectroscopy, pH metric titrations and the Boehm method. The IR spectra of CA-M and CA-N samples contain absorptions characteristic of unmodified activated carbons, whilst the IR spectra of the samples oxidized with nitric acid (CA-Mox) and nitric acid/urea mixture (CA-Mox-u and CA-Nox-u) display additional absorption bands, which are attributed to the OH group from alcohols, phenols and carboxylic acids. Moreover, the adsorption increases in intensity at $\sim 1700\text{ cm}^{-1}$ due to vibrations in the C=O bond of the carboxylic, ketones and aldehydes groups (Figure S2) [44–47].

The pH_{pzc} and dissociation constants of the functional groups (pK) on activated carbons surface were determined from the pH metric titrations. The obtained results show that the pH_{pzc} value of the studied activated carbons follows the series: CA-Mox (2.3) > CA-Mox-u (3.3) > CA-Nox-u (3.9) > CA-M (6.9) > CA-N (8.3) [24].

The curves of distribution of functional groups according to the pK value (Figure S3) show that both initial activated carbon samples (CA-N and CA-M) have only basic functional groups of 0.98 meq/g for the activated carbon CA-M and 0.75 meq/g for the activated carbon CA-N. In addition, it should be noted that most of the peaks belong to the CA-Mox sample (basic functional groups 0.45 meq/g and acid functional groups 1.33 meq/g) [48]. Four peaks are distinguishable for each of the activated carbon samples: CA-Mox-u (basic functional groups 0.58 meq/g and acidic functional groups 0.75 meq/g) and for CA-Nox-u (basic functional groups 0.60 meq/g and acidic functional groups 0.55 meq/g) [48].

The acidic or basic character of the functional groups on the surface of activated carbons determined by pH metric titrations is in good agreement with the type of functional groups determined via the Boehm method. Using the Boehm method [29,49], the following acidic groups have been identified on the surface of activated carbon: strongly carboxylic groups (CA-Mox, 0.95 meq/g; CA-Mox-u, 0.44 meq/g; CA-Nox-u, 0.32 meq/g), weakly carboxylic and phenolic groups (Table 3). The small discrepancies in values can be explained by different approaches in the determination of functional groups via these two methods.

Table 3. The quantity and character of functional groups (meq/g) on the surface of activated carbons, determined by the Boehm method.

Sample	The Amount of Functional Groups, meq/g				Character of Functional Groups, meq/g			
	Titrant				Carboxylic			
	0.05 N NaHCO ₃	0.1 N Na ₂ CO ₃	0.05 N NaOH	0.05 N HCl	Strong Acidic	Weak Acidic	Phenolic	Basic
CA-N	0.02 ± 0.03	0.07 ± 0.02	0.29 ± 0.03	0.92 ± 0.02	0.02	0.05	0.22	0.92
CA-M	0	0.35 ± 0.01	1.09 ± 0.01	0.98 ± 0.02	0	0.35	0.74	0.98
CA-Nox-u	0.32 ± 0.05	0.54 ± 0.01	0.86 ± 0.03	0.60 ± 0.02	0.32	0.22	0.32	0.60
CA-Mox-u	0.44 ± 0.04	0.77 ± 0.01	1.09 ± 0.05	0.55 ± 0.05	0.44	0.33	0.32	0.55
CA-Mox	0.95 ± 0.01	1.78 ± 0.02	1.9 ± 0.01	0.45 ± 0.03	0.95	0.83	0.12	0.45

3.2. Adsorption Studies

The kinetics of cobalt and strontium ions has been described using the following theoretical models: pseudo-first order, pseudo-second order and intraparticle diffusion (Weber–Morris model) models [36–39]. Figure 1 shows the kinetic curves of the adsorption process of cobalt ions on oxidized activated carbons (CA-Mox, CA-Mox-u and CA-Nox-u) and the pH value of the solutions. The concentration of cobalt(II) ions decreases rapidly to approx. 50–60 min of phase contact, after which the speed decreases until a relatively constant value is reached. The adsorption equilibrium of cobalt(II) ions on oxidized activated carbons (CA-Mox, CA-Mox-u and CA-Nox-u samples) is established for approx. 100 min, as seen from the kinetic curves of variation of the concentration of cobalt(II) ions in the solution, and the pH value of the solutions (Figure 1, Table 4). The adsorption of

cobalt ions on oxidized activated carbons is very well described by the pseudo-second-order kinetic model, since the calculated adsorption values are close to the experimental ones, and the value of the correlation coefficient (R^2) is close to 1 (0.999) compared to the R^2 obtained for the pseudo-first-order kinetic model (<0.921) (Tables 4 and S2). The mechanism of adsorption of cobalt ions on activated carbons, as described by the pseudo-second-order kinetic model, was also identified by other authors [50–52]. The applicability of the pseudo-second-order kinetic model suggests that the adsorption of cobalt ions on oxidized activated carbons is based on chemisorption, involving an exchange of electrons between the adsorbate and the adsorbent where the cobalt ions are attached to the activated carbon surface by chemical bonding [50–53].

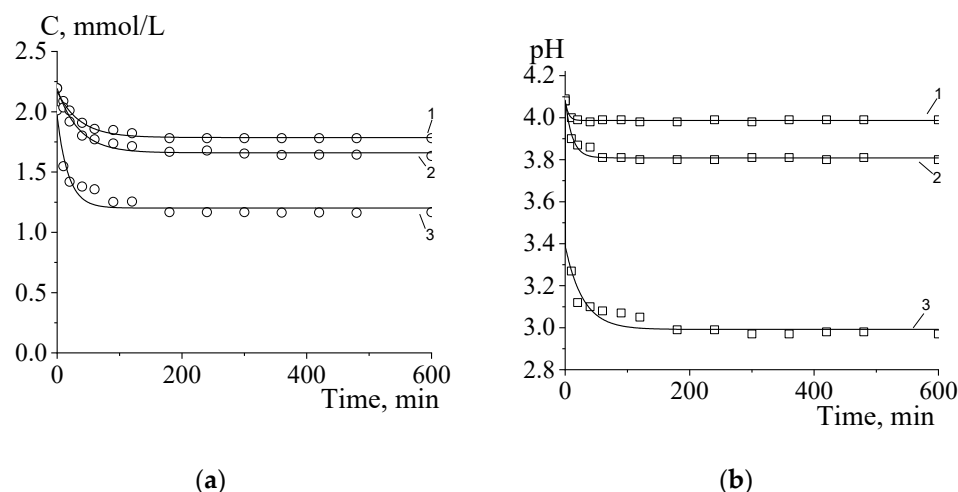


Figure 1. Kinetics of cobalt ions adsorption on oxidized activated carbons: (1) CA-Nox-u; (2) CA-Mox-u; (3) CA-Mox. (a) The variation of cobalt ions concentration in solution with time. (b) The pH value of solutions after adsorption of cobalt ions on activated carbons. Solid:liquid ratio—1:100, pH = 4.

Table 4. Kinetic parameters and q_e values of the adsorption process of cobalt ions ($C_0 = 2$ mmol/L) on oxidized activated carbons. Pseudo-second kinetic model (Ho and McKay).

Sample	q_e (exp), mmol/g	K_2 , g/mmol·min	q_e (cal), mmol/g	R^2
CA-Mox	0.085	0.914	0.087	0.999
CA-Mox-u	0.056	0.769	0.058	0.999
CA-Nox-u	0.041	1.327	0.043	0.999

The prediction of the rate-limiting step is an important factor to consider in the adsorption process. The adsorption mechanism could follow multiple kinetic orders that are changed during the adsorption process [54]. For adsorption at the solid/liquid interface, the solute transfer process is usually characterized by external mass transfer (diffusion into the solution film from the surface of the activated carbon particle) or intraparticle diffusion, or both. A better interpretation of the adsorption mechanisms can be obtained in the plots of q_t versus $t^{1/2}$. Figures 2 and S4 show the dependence of cobalt ions adsorption on the square root of time, according to the Weber–Morris model [39]. All the oxidized activated carbons showed a multilinearity of the lines, which implies that the adsorption process involves more than one kinetic stage (Figures 2 and S4). All the oxidized activated carbons showed a multilinearity of the lines, which implies that the adsorption process involves more than one kinetic stage (Figures 2 and S4). The first stage for the sample CA-Mox (Figure 2) suggests that the adsorption process proceeds through the stage of adsorption on the activated carbon particle surface (external adsorption), and the second

one corresponds to intraparticle diffusion (gradual diffusion within the pores). Then, the adsorption equilibrium has established [39].

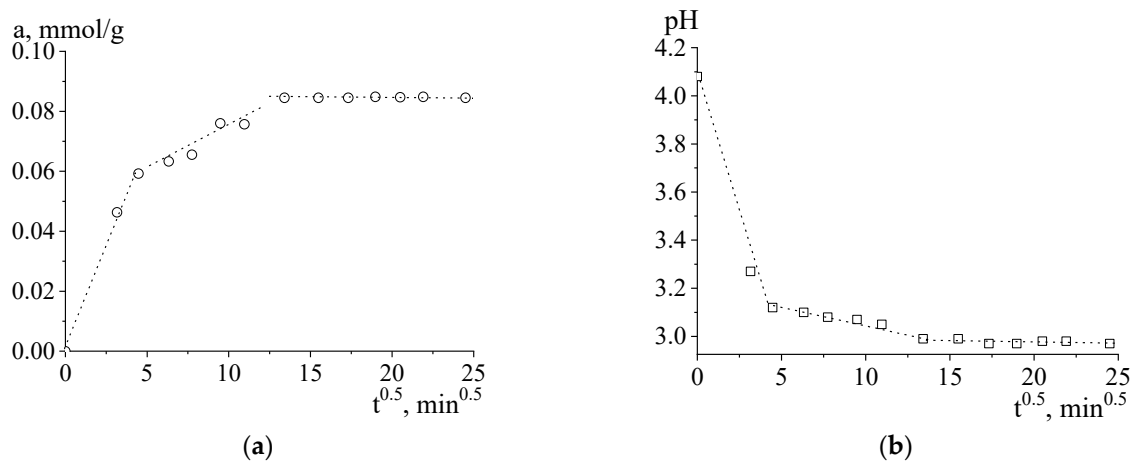


Figure 2. Intraparticle diffusion kinetic model (Weber–Morris) for cobalt ions adsorption on oxidized activated carbon CA-Mox. (a) The plot of a_t versus $t^{1/2}$; (b) the plot of pH_t versus $t^{1/2}$.

For the case of the strontium(II) ions adsorption from aqueous solutions (concentration of approx. 1 mmol/L) the adsorption equilibrium, both for the initial activated carbons (CA-N, CA-M) and for the oxidized activated carbons (CA-Nox-u, CA-Mox-u, CA-Mox), is established after approx. 100 min (Figures 3 and S5–S7). The pH value of the strontium solution after contact with CA-M activated carbon increases from 4.0 to 5.2 (Figure 3b), also on the dependence 2 inflections are observed. Such inflections were also observed by other authors, who assume that the adsorption of strontium ions takes place in several steps [55]. Among the oxidized activated carbon samples, as in the case of cobalt ions adsorption, the CA-Mox sample is distinguished, which shows the highest adsorption capacity for strontium ions (Figure 3, Table 5). The behavior of oxidized activated carbons (CA-Mox, CA-Mox-u and CA-Nox-u) in strontium(II) solutions is interesting, as the sample CA-Mox tends to decrease the pH value from 4.0 to 3.5 in the first minutes of contact and gradually increases up to approx. 3.7, which corresponds to the adsorption equilibrium establishing time (Figure 3b). For CA-Mox-u and CA-Nox-u samples, the pH value increases from 4.0 to 4.5 and 5.7, respectively (Figures S6 and S7). This suggests that the pH value of the solution tends towards the pH_{pzs} value of activated carbons.

The adsorption of strontium ions on the studied activated carbons is described by the pseudo-second-order kinetic model; the calculated adsorption value is close to that determined experimentally, and the correlation coefficients for the initial and oxidized activated carbons are close to 1, in contrast to the pseudo-first-order kinetic model ($R^2 = 0.524–0.915$) (Tables 5 and S3). According to the data published in the specialized literature, the kinetics of the adsorption process of strontium ions on activated carbons is best described by the pseudo-second-order kinetic model [56–58].

The kinetic adjustment of the experimental data with the intraparticle diffusion model (Weber–Morris) pointed out that the adsorption process of strontium ions on activated carbons takes place in two stages: the first stage, linear for sample CA-M and curved for CA-Mox, is followed by a second linear stage and the curves do not pass through the origin (Figure 4). These two steps of the intraparticle diffusion model suggest that the adsorption process proceeds through the sorption of strontium(II) ions on the activated carbon surface and intraparticle diffusion. The initial curved portion of the dependence indicates the effect of the solution layer or film on the surface of the adsorbent particles, while the second, linear portion is due to intraparticle or pore diffusion [59].

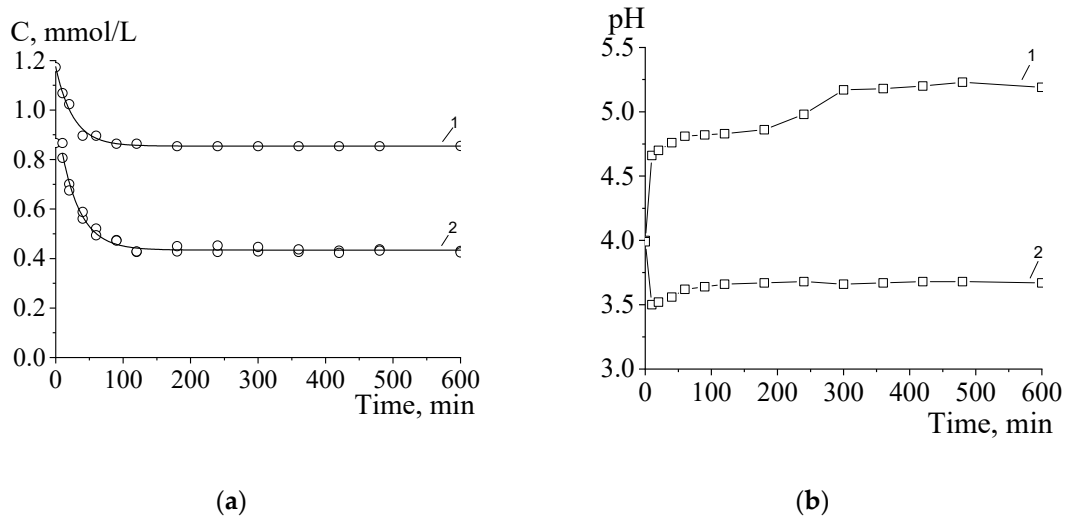


Figure 3. Kinetics of strontium ions adsorption on activated carbons: CA-M (1) și CA-Mox (2). (a) The variation of strontium ions concentration in solution with time. (b) The pH value of solutions after adsorption of strontium ions on activated carbons. Solid:liquid ratio—1:100, pH = 4.

Table 5. Kinetic parameters and q_e values of the adsorption process of strontium ions ($C_0 = 1$ mmol/L) on activated carbons. Pseudo-second-order kinetic model (Ho and McKay).

Sample	q_e (exp), mmol/g	K_2 , g/mmol·min	q_e (cal), mmol/g	R^2
CA-M	0.032	2.372	0.033	0.999
CA-N	0.034	2.138	0.035	0.991
CA-Mox	0.076	1.562	0.077	0.999
CA-Mox-u	0.041	1.478	0.043	0.999
CA-Nox-u	0.034	1.894	0.035	0.999

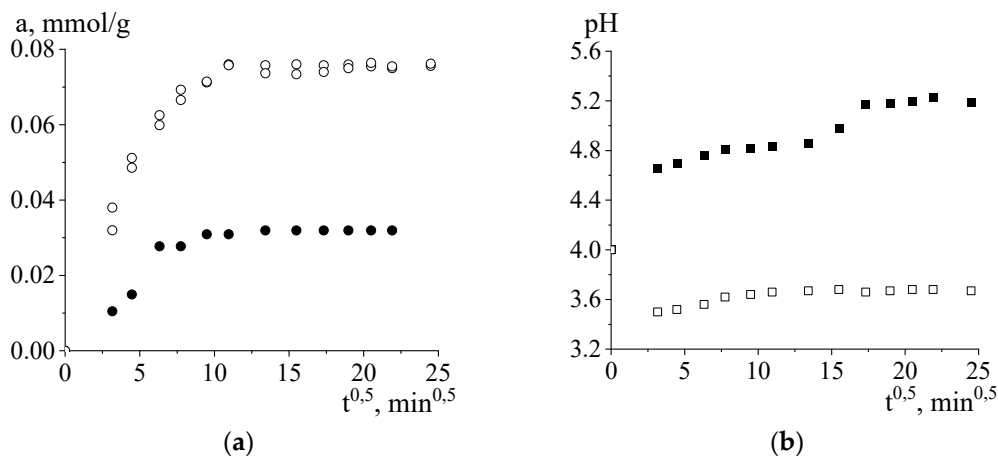


Figure 4. Intraparticle diffusion kinetic model (Weber–Morris) for strontium ions adsorption on activated carbons CA-M (●, ■) and CA-Mox (○, □). (a) The plot of a_t versus $t^{1/2}$, (b) the plot of pH_t versus $t^{1/2}$.

The results of the adsorption equilibrium data of the cobalt(II) and strontium(II) ions were fitted with theoretic models Langmuir, Freundlich, Temkin–Pyzhev and Dubinin–Radushkevich. The experimental data for the cobalt ions adsorption on oxidized activated carbon samples (CA-Mox, CA-Mox-u and CA-Nox-u) are best described by the Langmuir isotherm model (Figure 5 and Table 6) and also correlate well with data from the literature.

According to adsorption isotherms, the CA-Mox sample adsorbs approx. 0.079 mmol/g, CA-Mox-u approx. 0.051 mmol/g and CA-Nox-u approx. 0.038 mmol/g of cobalt ions. The R^2 value of the four theoretical models applied to describe the adsorption of cobalt(II) ions on oxidized activated carbons decreases in the order: Langmuir > Temkin–Pyzhev > Dubinin–Radushkevich > Freundlich. It is clear that the Langmuir model corresponds to a dominant electrostatic attraction, ion exchange and complexation mechanism, while the order of the models shows that the adsorption process involved the physical adsorption and complexation process at the external heterogeneous surface of oxidized activated carbons.

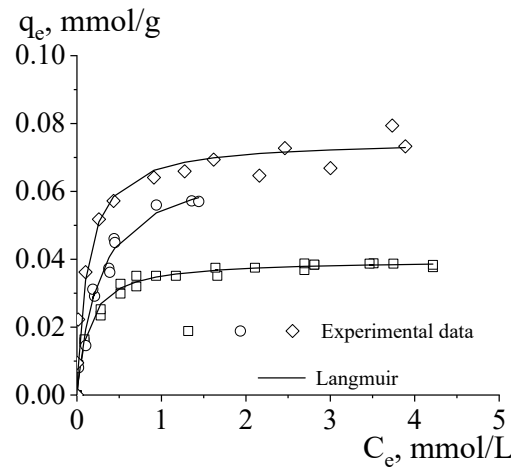


Figure 5. Adsorption isotherms of cobalt ions on oxidized activated carbons: (◇) CA-Mox, (○) CAMox-u and (□) CA-Nox-u. Solid:liquid ratio—1:100, pH 4.

Table 6. Langmuir, Freundlich, Temkin–Pyzhev and Dubinin–Radushkevich isotherm constants for the adsorption of cobalt ions on oxidized activated carbons.

Isotherm Model	Parameters	CA-Mox	CA-Mox-u	CA-Nox-u
Langmuir	K_L (L/mmol)	8.096	3.768	7.357
	Q_0 (mmol/g)	0.075	0.069	0.040
	R^2	0.989	0.979	0.999
R_L		$6.1 \times 10^{-6} \div 1.6 \times 10^{-5}$	$1.2 \times 10^{-5} \div 1.6 \times 10^{-5}$	$6.1 \times 10^{-6} \div 2.2 \times 10^{-4}$
Freundlich	K_f (mmol/g)	0.059	0.057	0.031
	n	3.88	2.08	4.12
	R^2	0.941	0.935	0.891
Temkin–Pyzhev	K_T (L/g)	974.7	56.8	298.5
	B_T	0.009	0.013	0.006
	R^2	0.970	0.923	0.938
Dubinin–Radushkevich	K_{ads} (mol ² /kJ ²)	9.23×10^{-9}	2.24×10^{-8}	1.67×10^{-8}
	Q_0 (mmol/g)	0.067	0.051	0.037
	E (kJ/mol)	7.36	4.725	5.472
	R^2	0.955	0.870	0.922

The maximum monolayer adsorption capacity of oxidized activated carbons for cobalt(II) ions (calculated according to the Langmuir model) is 0.075 mmol/g for the CA-Mox sample, 0.069 mmol/g for the CA-Mox-u sample and 0.040 mmol/g for the CA-Nox-u sample (Table 6). For all oxidized activated carbons (CA-Mox, CA-Mox-u and

CA-Nox-u) the R_L value fell within the limits of $6.1 \times 10^{-6} \div 2.2 \times 10^{-4}$, which means that the process of adsorption of cobalt(II) ions on the studied samples is very favorable [14,50–52]. The free energy calculated according to the Dubinin–Radushkevich model denotes that chemical sorption takes place in the modeled system (Table 6).

Acidic functional groups on the surface of activated carbons play an important role in the adsorption of metal ions from solutions [13,14,51,60]. When contacting activated carbon with an aqueous solution, the acidic functional groups on the surface are ionized, H^+ ions are released into the solution and the activated carbon surface becomes negatively charged, on the surface appear negatively charged adsorption centers [61]. The greater the number of acidic groups on the surface of the activated carbon, the more negative the charge on the surface of the activated carbon will be. This leads to increased electrostatic attraction between the negatively charged activated carbon surface and the positively charged metal cations [13,14,23,61].

The pH value of the cobalt nitrate solution after contact with the oxidized activated carbons decreases due to the acid functional groups on the surface and their ionization effect. For the CA-Mox sample, the pH value of cobalt(II) solutions at equilibrium gradually decreases from approx. 4 to approx. 3, when the adsorption equilibrium of cobalt ions is also reached, and for the CA-Mox-u and CA-Nox-u samples the pH value of the solutions drops to 3.8, indicating the fact that adsorption occurs by ion exchange (Figure S8).

In the case of the adsorption of strontium(II) ions from the solution on the oxidized activated carbons, from the adsorption isotherms it is observed that the activated carbon CA-Mox adsorbs about 0.073 mmol/g, the activated carbon CA-Mox-u adsorbs approx. 0.033 mmol/g and CA-Nox-u adsorbs 0.028 mmol/g of strontium ions (Figure 6).

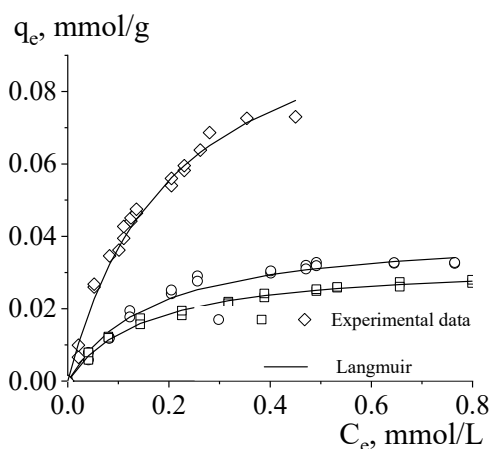


Figure 6. Adsorption isotherms of strontium ions on oxidized activated carbons: (\diamond) CA-Mox, (\circ) CAMox-u and (\square) CA-Nox-u. Solid:liquid ratio—1:100, pH 4.

The pH value of the equilibrium solutions also differs for the strontium nitrate solutions after contact with CA-Mox, as the pH value at the lowest equilibrium concentrations gradually decreases from 4 to approx. 3.6 and to approx. 3.4 around reaching equilibrium (Figure S9). In the case of the adsorption isotherms of strontium ions on CA-Mox-u and CA-Nox-u samples in equilibrium solutions, the pH trend is totally different. The pH value from 4.0 (in the initial solutions) increases to 5.8 and then gradually decreases to approx. 4.6 for the CA-Mox-u sample, and for the CA-Nox-u sample the pH value increases from 4.0 to 6.2 and decreases to approx. 5.8, upon reaching equilibrium (Figure S9) [24]. Although the results obtained for the pH value of the equilibrium solutions for the CA-Mox-u and CA-Nox-u samples seem to contradict those obtained for the CA-Mox sample, they are consistent with the pH value of the solutions at reaching equilibrium to study the adsorption kinetics of strontium ions.

The parameters and constants of the theoretical isotherms calculated for the adsorption of strontium(II) ions on the oxidized activated carbons CA-Mox, CA-Mox-u and CA-

Nox-u are presented in Table 7. According to the correlation coefficients, the adsorption isotherms of strontium(II) ions on oxidized activated carbons correspond to the Langmuir model. According to data from the literature, the adsorption process of strontium(II) ions on activated charcoal from rice straw (non-oxidized) is described by the Dubinin–Radushkevich model; at the same time, the authors say that the adsorption is a physical one, with a free energy of 9.7 kJ/mol [56]. Similar results of applicability of the Dubinin–Radushkevich model for describing the adsorption of strontium(II) ions on modified activated carbons are presented for a limited range of equilibrium concentrations 0.016–0.084 mmol/L [60].

Table 7. Langmuir, Freundlich, Temkin–Pyzhev and Dubinin–Radushkevich isotherm constants for the adsorption of strontium ions on oxidized activated carbons.

Isotherm Model	Parameters	CA-Mox	CA-Mox-u	CA-Nox-u
Langmuir	K_L (L/mmol)	4.798	6.081	6.578
	Q_0 (mmol/g)	0.077	0.041	0.033
	R^2	0.904	0.978	0.995
R_L		0.15 ÷ 0.68	0.12 ÷ 0.62	0.11 ÷ 0.60
Freundlich	K_f (mmol/g)	0.175	0.047	0.034
	n	1.40	1.90	2.24
	R^2	0.916	0.888	0.931
Temkin–Pyzhev	K_T (L/g)	61.9	53.9	67.4
	B_T	0.022	0.009	0.007
	R^2	0.984	0.954	0.988
Dubinin–Radushkevich	K_{ads} (mol ² /kJ ²)	2.7×10^{-8}	2.8×10^{-8}	2.3×10^{-8}
	Q_0 (mmol/g)	0.095	0.039	0.030
	E (kJ/mol)	4.30	4.23	4.663
	R^2	0.978	0.977	0.979

The R_L value demonstrates that the adsorption process of strontium(II) ions on oxidized activated carbons is favorable, also being confirmed with the help of the empirical parameter ($1/n$) calculated for the theoretical Freundlich model ($0 < 1/n < 1$). The free energy calculated according to the Dubinin–Radushkevich model identifies that in the modeled system a chemical sorption occurs.

By summarizing the obtained results, the adsorption capacity of the studied activated carbons (CA-Mox, CA-Mox-u and CA-Nox-u) for both cobalt(II) and strontium(II) ions, determined from kinetics measurements and adsorption isotherms correlates well. The data from the literature regarding the maximum adsorption capacities of different carbonaceous adsorbents for cobalt(II) and strontium(II) ions removal are summarized in Table S5. These results show that the adsorption capacity of CA-Mox, CA-Mox-u and CA-Mox-u for adsorption of cobalt(II) and strontium(II) are comparative to some adsorbents and lower with others, but it is quite challenging to draw a conclusion because the experimental conditions are very different (regarding initial concentration, pH value temperature, etc.).

In some research, several factors influencing the adsorption of metal ions on adsorbents are discussed, such as ion radius, hydrated ion radius, hydration energy, and electronegativity [53,57,62]. In general, the larger the radius of the ion, the greater the affinity for the adsorbent surface.

Metal cations with lower hydration energy will have a greater tendency to be adsorbed on activated carbons [53]. Ions with a higher electronegativity will be more tightly attracted to the surface of the adsorbent [53]. In aqueous solutions cobalt(II) and strontium(II) ions

are hydrated; cobalt(II) ions are surrounded by six water molecules $[\text{Co}(\text{H}_2\text{O})_6]^{2+}$ and strontium ions are octahydrated $[\text{Sr}(\text{H}_2\text{O})_8]^{2+}$ [62,63]. The radii of hydrated cobalt(II) and strontium(II) ions are very close in value, 0.412 nm and 0.423 nm, respectively (Table S4). At the same time, the hydration-free energy is lower for cobalt(II) ions, and the electronegativity is higher, which means that cobalt(II) ions will have a higher affinity [63] to the activated carbon surface (Table S4). Under the conditions of the experiments in the paper, according to the obtained data, the adsorption capacity of activated carbons for cobalt(II) ions is comparable to that for strontium(II) ions.

The pH value is an important parameter for the adsorption of metal ions from aqueous solutions because it affects the metal ions solubility, the concentration of ions associated with the adsorbent functional groups and the ionization degree of functional groups during the reaction [64]. In cases when the solution pH is higher than the adsorbent pH_{pzc} , the negative charge from the surface ensures favorable electrostatic interactions for the cationic species adsorption. For the samples of activated carbons used in the Co(II) and Sr(II) ions adsorption from aqueous solutions, the pH_{pzc} value increases as follows: CA-Mox (2.3) > CA-Mox-u (3.3) > CA-Nox-u (3.9) > CA-M (6.9) > CA-N (8.3).

The pH influence on the adsorption (removal) of cobalt(II) and strontium(II) ions from the solution in the presence of activated carbons is represented in Figure 7, Figures S9 and S10. It should be noted that the values of pH and electrical conductivity of the final solutions are different than those of the initial solutions. In the case of cobalt(II) ions removal, the pH of initial solutions varies from 1 to 10 (the conductivity value ranges from 118 to 128 μScm^{-1}), while pH at equilibrium varies in steps. As shown in Figure 7 and Figure S9, for the removal rate of cobalt(II) ions (variation of pH and conductivity at equilibrium), the behavior of initial activated carbons, CA-M and CA-N, and the oxidized ones, CA-Mox-u and CA-Nox-u, is similar: nothing happens on the pH range from 1 to 2, the pH value is constant and the cobalt ions removal rate is null. This fact is also demonstrated by the conductivity of the solutions.

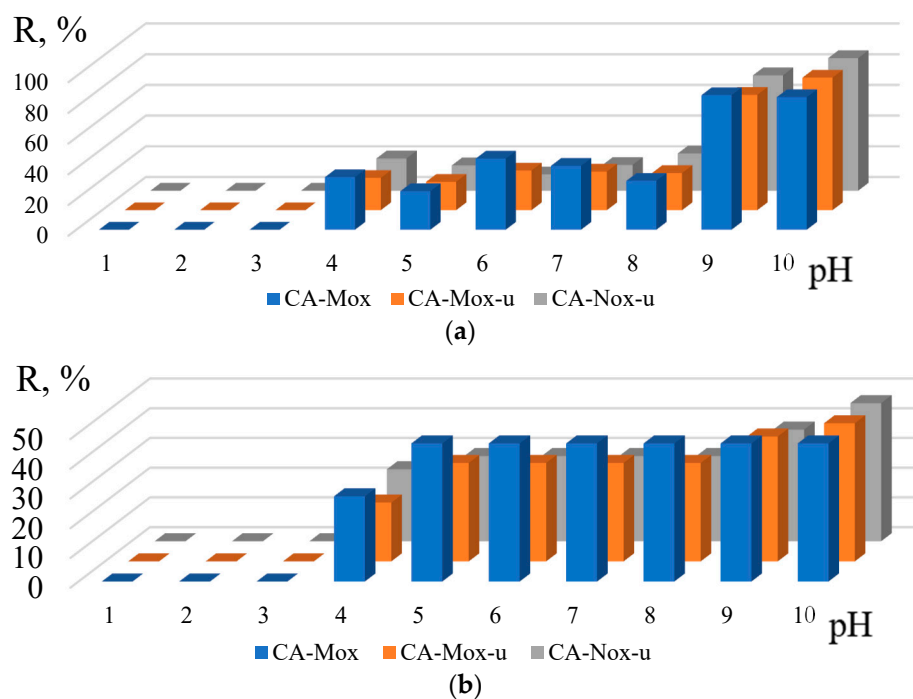


Figure 7. The pH influence on the adsorption (removal) of cobalt(II) and strontium(II) ions from the solution in the presence of oxidized activated carbons. Removal rate (R, %) of cobalt(II) ions (a) and strontium(II) ions (b) from solutions.

On the second pH interval 3–5, the equilibrium pH varies between 3.25–3.70. On the same interval, one observes an increase in the removal rate of cobalt ions, comparable

values for these four types of activated carbons (CA-M, CA-N, CA-Mox-u and CA-Nox-u). It is unclear if acidic functional groups from the activated carbon surface were involved in the cobalt ions adsorption. The pH_{pzc} value of the oxidized samples is 3.3 (CA-Mox-u) and 3.9 (CA-Nox-u) and in this pH of solutions, some acidic functional groups from the oxidized activated carbon surface should be ionized. For solutions with an initial pH of 6, the value of pH at equilibrium suddenly increases up to ~ 6.8 . This phenomenon can be explained by the presence of various forms of cobalt ions in solution, e.g., $\text{Co}(\text{OH})^+$, $\text{Co}(\text{OH})_2$ and $\text{Co}(\text{OH})_3^-$, at pH near 8; therefore, the effect of cobalt ions removal is decreased (Figure S12) [50]. For the next stage (pH 7–10), the initial pH of the solutions decreases to 7.0–7.5 at equilibrium. On this interval, most probably, the precipitation of cobalt ions takes place but not the adsorption, because the conductivity value is nearly constant in these solutions (Figure 8). On the diagram of cobalt ions removal from solution, at pH values of 9 and 10 the removal rate increases until $\sim 85\%$. However, this is due to the precipitation of the cobalt ions in the hydroxide form (Figure 7a). The influence of the solution pH on cobalt ions adsorption on various adsorbents had been studied by several researchers. Nevertheless, the pH interval when cobalt ions adsorption occurs is different and some have reported that maximum adsorption occurs in the pH interval 3–5, 6.5 and 7 [50,52,65–68].

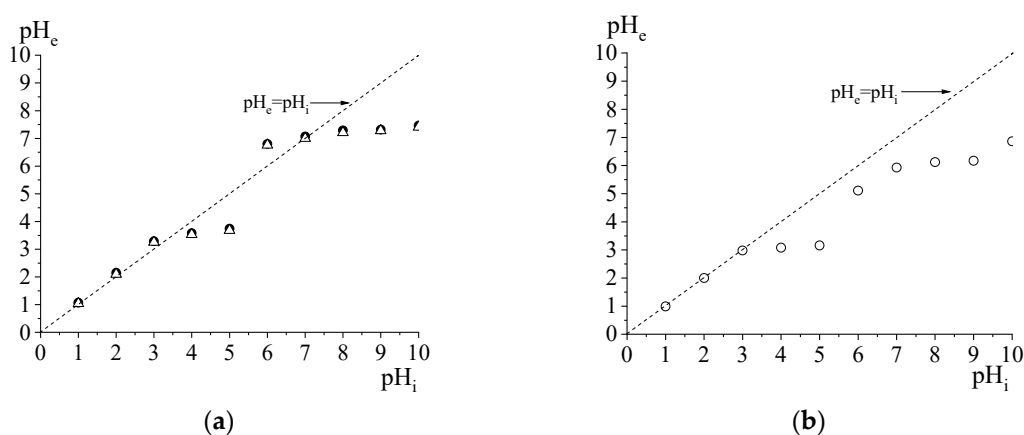


Figure 8. The pH influence on the adsorption (removal) of cobalt(II) ions from solutions in the presence of oxidized activated carbons: Δ CA-Nox-u, \bullet CA-Mox-u, \circ CA-Mox. (a) and (b) pH variation in equilibrium solutions.

The oxidized activated carbon CA-Mox, when compared to other samples, behaves slightly differently in solution. On the pH interval 1–2, the pH value at equilibrium remains constant, and the removal rate of cobalt ions is null (Figure 8). With the increase in the initial solution pH (pH interval 3–5), the pH at equilibrium decreases to ~ 3 (2.98–3.16). This pH interval is higher than the pH_{pzc} of this activated carbon (2.3) and the cobalt ions adsorption depends on the dissociation state of weak acidic functional groups. At pH higher than 5, the number of competitive hydrogen ions is lower and more functional groups are dissociated, the charge on the surface of the activated carbon CA-Mox becomes more negative and, therefore, contributes to the cobalt ions adsorption via ion exchange. For solution pH of 6, the pH at equilibrium decreases to 5.1 (Figure 8b), also, the increase in the adsorption rate of cobalt ions is observed (Figure 7a). This can be explained by two effects: (i) at pH 6, the dissociation of strong acidic functional groups from the surface of CA-Mox begins, hydrogen ions are released in solution (solution pH decreases) and adsorption of cobalt cations occurs; (ii) $\text{pH } 6 > \text{pH}_{\text{pzc}}$ of activated carbon CA-Mox, then the surface is more negatively charged and attracts positively charged cobalt ions. From Figure 8, the variation of the pH value at equilibrium (and of the conductivity [24]), it is highlighted that cobalt ions adsorption occurs up to pH 8 of the initial solutions (equilibrium pH of 5.9–6.1) (Figure 7a).

Generally, functional groups from the activated carbons' surface possess affinity and adsorption capacity for heavy metal ions because they are able to donate a pair of electrons, thus bonding the metal via chelation or complexation. The adsorption mechanism is explained by surface complexation, diffusion in adsorbent micropores, chemisorption, ion exchange and electrostatic interactions, which may occur in the singular or complex modes [13,69].

The obtained results show that acidic functional groups formed on the activated carbon surface CA-Mox (via oxidation with nitric acid) had led to the increase in the ion exchange capacity among the cobalt(II) ions and the following functional groups: hydroxyl (-OH), carboxyl (-COOH) and carbonyl (-C=O). Other researchers have also tried to explain a dependence between the point of zero charge (PZC), solutions pH and the character of surface functional groups [14,68,70]. The studies have revealed that the modification of the solution pH leads to the change of the activated carbon surface charge, which is different for different solution pH values [68,71]. It is also mentioned that carboxylic and lactone groups dissociate in aqueous solutions, the H^+ ions transfer in the solution and the activated carbon surface remains negatively charged ($-COO^-$) [68,72].

In the case of strontium(II) ions adsorption onto activated carbons (CA-M, CA-N, CA-Mox-u, CA-Nox-u and CA-Mox), the adsorption capacity depends on the solution's pH value. At an initial solution $pH < 3$, the value of pH at equilibrium is not modified for all the investigated samples, and the strontium ions adsorption does not occur, which suggests the complete protonation of the functional groups from the activated carbon surface (Figure 8b and Figure S11). For higher pH values (4–7), the removal rate of strontium ions from the solution is increased; this observation is in agreement with the conductivity value at equilibrium for this pH range. On the pH interval $8 \div 10$ of the initial solution, the removal rate of strontium ions slightly increases, but the pH value at equilibrium remains constant at around 6 for CA-M, CA-N, CA-Mox-u and CA-Nox-u carbons and in the range of 4 and 5 for CA-Mox. For all samples of activated carbons, the solution conductivity at equilibrium tends to decrease. In aqueous solutions, strontium is found as Sr^{2+} ions and $SrOH^+$ species on a broad pH interval (pH 6–10, Figure S13), but $SrOH^+$ is the main form at $pH > 12.8$ [63]. The strontium ions removal capacity at pH higher than 7 may be due to a combined effect of adsorption and precipitation on the activated carbon surface [73].

Generally, according to the results obtained, there is not a good agreement between the amount of acid functional groups on the surface of oxidized activated carbons (determined by the Boehm method and electrometric titrations) and the amount of adsorbed metals. This was also observed by other authors and can be explained by the fact that not all acidic functional groups are accessible to hydrated metal ions. The acidic functional groups in the pores often interact with each other and block the pores [13].

In the literature, for the adsorption of strontium ions from solutions on activated carbon from rice straw, modified chitosan, activated carbon obtained from almond shells and activated carbon from pecan nuts, the ion exchange mechanism between carboxylic, phenolic and lactone acidic functional groups has been proposed and strontium ions [57,58,73–75] or the combination of two mechanisms, dipole–dipole interaction and ion exchange [60].

3.3. The Suggested Mechanisms for the Adsorption of Co(II)/Sr(II) Ions on Activated Carbons

By corroborating the obtained results regarding the characterization of carbonaceous adsorbents surface chemistry and the metal ions' adsorption capacity as a function of the solution pH, mechanisms of adsorption are proposed.

For the metal ions' adsorption onto activated carbons at $pH < 3$, there is competition between the H^+ and Me^{2+} ions for the same adsorption site.

The interval $pH < pH_{pzc}$ of activated carbons. Generally, at values of $pH < pH_{pzc}$, the metal ions' adsorption on activated carbons may occur via the complexation mechanism (between the oxygen atoms from C=O groups from the activated carbon surface and the metal ions) and electrostatic interactions (Figure 9).

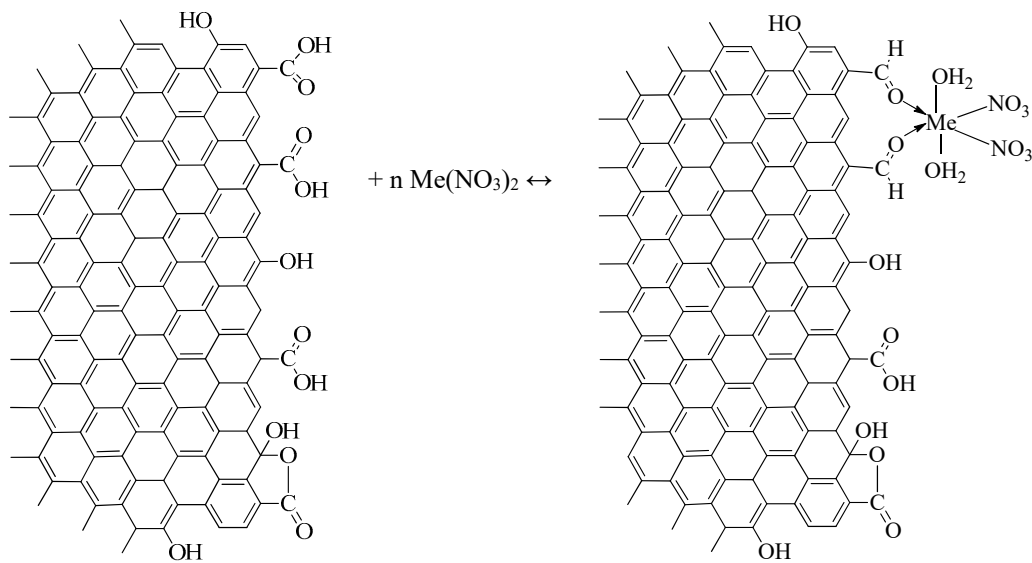


Figure 9. Schematic presentation of the adsorption of metal ions on activated carbons by complexation.

The interactions $C_{\pi}-Me^{n+}$ (cation) are attributed to electrostatic interactions between the aromatic rings of carbonaceous adsorbents (with the basic surface) and metal cations. On the activated carbon surface, according to some authors, the π (C_{π}) electrons possess weak negative charge properties [76]. The positions with C_{π} electronic density could correspond to the basic functional groups determined via the Boehm method (chromene, ketones and pyrones structures) [76].

- *The interval of pH 3 ÷ 5.* In this pH interval, the oxidized activated carbons adsorb metal ions by ion exchange and the formation of metal–ligand complexes on the surface (Figure 10).

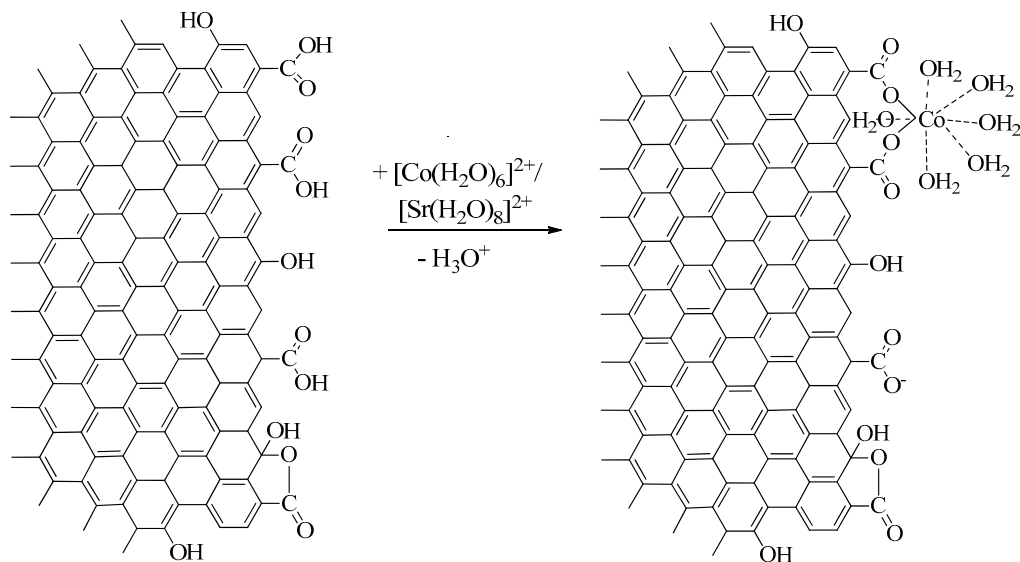


Figure 10. Schematic presentation of the adsorption of metal ions on oxidized activated carbons by ion exchange and the formation of metal–ligand complexes on the surface.

- *The pH interval of 5 ÷ 7.* For oxidized activated carbon, within this interval, the weak acidic functional groups dissociate, e.g., lactones. At the same time, the species of $Co(II)$, $Co(OH)^+$, $Co(OH)_2$ and $Co(OH)_3^-$ begin to form in the solution. The schematic

presentation of the adsorption of Co(II) ion species on the surface of oxidized activated carbon by ion exchange and complexation is shown in Figure 11.

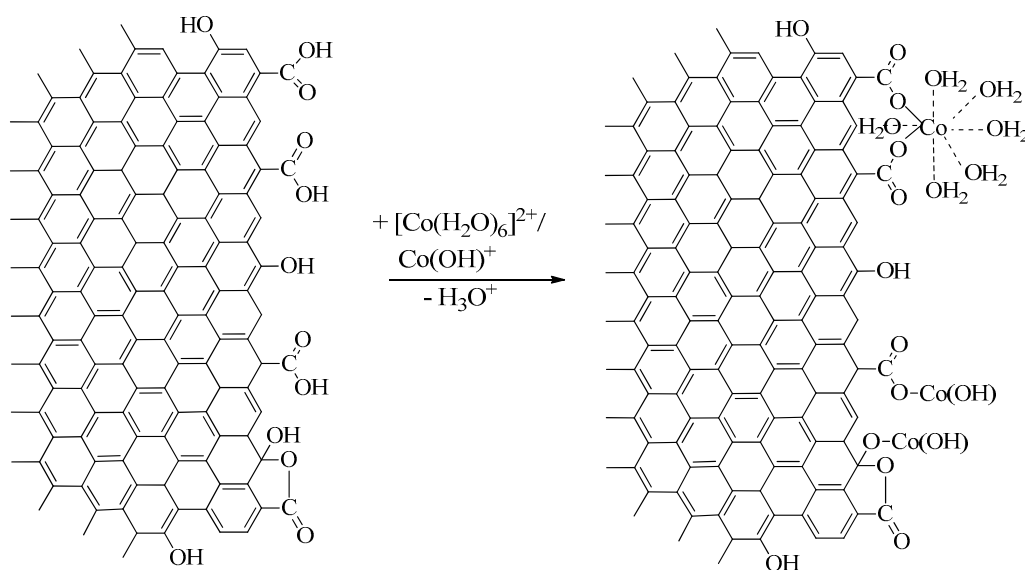


Figure 11. Schematic presentation of the adsorption of Co(II) ion species on the surface of oxidized activated carbon by ion exchange and complexation.

The interval of $pH > 7$. For oxidized activated carbons, within this interval, the dissociation of hydroxyl groups (from phenols and alcohols, $-OH$; $pK \sim 9-13$) begins, also in this interval $Co(OH)_2$ and $Sr(OH)_2$ hydroxides are formed. Moreover, the increase in the removal rate of Co(II) and Sr(II) ions is mostly due to the precipitate formation of these hydroxides in solution or on the activated carbon surface. In conclusion, under the modeled conditions, for the studied metal ions, hydroxyl groups do not participate in the adsorption process.

4. Conclusions

New carbonaceous adsorbents had been obtained from walnut shells and apple wood by modifying the surface via oxidation with nitric acid and nitric acid/urea mixture. The presence of functional groups on the surface of activated carbons obtained from nut shells and apple wood has been determined by using IR spectroscopy, pH metric titrations and the Boehm method. The following functional groups have been identified on the surface of activated carbon: strongly acidic groups (CA-Mox, 0.95 meq/g; CA-Mox-u, 0.44 meq/g; CA-Nox-u, 0.32 meq/g) and weakly acidic and phenolic groups, while the pH_{pzc} value of the studied activated carbons increase as follows: CA-Mox (2.3) > CA-Mox-u (3.3) > CA-Nox-u (3.9) > CA-M (6.9) > CA-N (8.3).

The adsorption process of strontium(II) and cobalt(II) ions on activated carbons has been studied by applying the following models: pseudo-first-order model, pseudo-second-order model and intraparticle diffusion model, as well as theoretic isotherms models of Langmuir, Freundlich, Temkin–Pyzhev and Dubinin–Radushkevich. The experimental data are best described by the pseudo-second kinetic model suggesting that the adsorption of metal ions (cobalt(II) and strontium(II)) onto oxidized activated carbons is based on chemisorption. The constants determined for the Freundlich and Langmuir models and the energy values estimated by Dubinin–Radushkevich demonstrate that the adsorption process of strontium(II) and cobalt(II) ions onto oxidized activated carbons is favorable and dominated by chemisorption of the energetically homogenous surface in the modeled system.

The investigations highlight the important role of the solution pH, of the activated carbons functional groups and the pH_{pzc} value for the adsorption process of cobalt(II) and

strontium(II) ions. It should be noted that depending on the surface chemistry and solution pH, the adsorption of strontium(II) and cobalt(II) ions occurs via different mechanisms:

- For $\text{pH} < \text{pH}_{\text{pzc}}$ values, the adsorption of metal ions on activated carbons may occur through the complexation mechanism (between oxygen atoms from C=O groups from the activated carbon surface and metal ions) and electrostatic interactions;
- For the adsorption of metal ions on initial activated carbons (with the basic surface, on the pH interval $3 \div 5$), the mechanism of adsorption via electrostatic interactions between the $\text{C}\pi$ sites and metal ions has been proposed. For oxidized activated carbons, the mechanism of ion exchange between the carboxylic groups and metal ions and the formation of metal–ligand complexes on the surface has been proposed;
- Within the pH interval $5 \div 7$, the weak acidic functional groups of lactone type dissociate and the mechanism of adsorption of cobalt(II) ion species on the surface of the oxidized activated carbon via ion exchange and complexation has been proposed.

Supplementary Materials: The following supporting information can be downloaded at: <https://www.mdpi.com/article/10.3390/c9030071/s1>, Table S1: The metal quantity (%) in activated carbons, recalculated to oxides. Figure S1: SEM-EDX profiles for activated carbons: (a) CA-N; (b) CA-M; (c) CA-Nox-u; (d) CA-Mox-u; (e) CA-Mox. Figure S2: FTIR spectra of activated carbons: (1) CA-M; (2) CA-N; (3) CA-Mox; (4) CA-Mox-u; (5) CA-Nox-u. Figure S3: Distribution of surface groups according to the dissociation constants pK [1]. Table S2: Kinetic parameters and q_e values of the adsorption process of cobalt ions ($\text{C}_0 = 2 \text{ mmol/L}$) on oxidized activated carbons. Figure S4: Intraparticle diffusion kinetic model (Weber–Morris) for cobalt ions adsorption on oxidized activated carbon CA-Mox-u. (a) The plot of a_t versus $t^{1/2}$, (b) the plot of pH_t versus $t^{1/2}$. Figure S5: Kinetics of strontium ions adsorption on initial activated carbon CA-N. (a) The variation of strontium ions concentration in solution with time; (b) the pH value of solutions after adsorption of strontium ions on activated carbon. Solid:liquid ratio—1:100, pH = 4. Figure S6: Kinetics of strontium ions adsorption on oxidized activated carbon CA-Mox-u. (a) The variation of strontium ions concentration in solution with time; (b) the pH value of solutions after adsorption of strontium ions on activated carbon. Solid:liquid ratio—1:100, pH = 4; Table S3: Kinetic parameters and q_e values of the adsorption process of strontium ions on activated carbons. Figure S8: The pH value of solution at equilibrium for adsorption isotherms of cobalt ions on oxidized activated carbons: (\diamond) CA-Mox, (\circ) CAMox-u and (\square) CA-Nox-u. Solid:liquid ratio—1:100, pH 4. Figure S9: The pH value of solution at equilibrium for adsorption isotherms of strontium ions on oxidized activated carbons: (\diamond) CA-Mox, (\circ) CAMox-u and (\square) CA-Nox-u. Solid:liquid ratio—1:100, pH 4. Table S4: Ions properties (selective) [1]. Table S5: Comparison of the adsorption capacity of the studied activated carbons with other carbonaceous adsorbents used for the removal of Co(II) and Sr(II) ions. Figure S10: The pH influence on the adsorption (removal) of cobalt(II) ions from the solution in the presence of initial activated carbons. (a) Removal rate (%); (b) pH of equilibrium solutions for \bullet CA-M. and Δ CA-N; (c) conductivity of equilibrium solutions for \bullet CA-M. and Δ CA-N. Figure S11: The pH influence on the adsorption (removal) of strontium(II) ions from the solution in the presence of initial activated carbons. (a) Removal rate (%); (b) pH of equilibrium solutions for \bullet CA-M. and Δ CA-N; (c) conductivity of equilibrium solutions for \bullet CA-M. and Δ CA-N. Figure S12: Equilibrium mass distribution of Co species as a function of pH. $\text{C}_0(\text{Co}(\text{NO}_3)_2) = 0.05 \text{ mmol/L}$, temperature $25 \text{ }^\circ\text{C}$. Figure S13: Equilibrium mass distribution of Sr species as a function of pH. $\text{C}_0(\text{Sr}(\text{NO}_3)_2) = 0.05 \text{ mmol/L}$, temperature $25 \text{ }^\circ\text{C}$. Appendix S1: The scheme of the activated carbon oxidation installation. Appendix S2: The explanation of the urea role in the oxidation process of activated carbons with the mixture of nitric acid/urea [1]. Appendix S3: Boehm selective neutralization technique. Appendix S4: Acid-base properties.

Author Contributions: I.C.: investigation, methodology, validation, formal analysis and visualization; T.L.: project administration, supervision and visualization; S.M.: data discussions and editing; R.N.: conceptualization, supervision, methodology, investigation, validation, formal analysis, visualization, writing—original draft and writing—review and editing. All authors have read and agreed to the published version of the manuscript.

Funding: This research was funded by H2020 MSCA-RISE-2016/NanoMed Project, grant number 734641 and the Republic of Moldova Project “Reducing the Impact of Toxic Chemicals on the Environ-

ment and Health by Using Adsorbents and Catalysts Obtained from Local Raw Materials”, DISTOX, no. 20.80009.7007.21.

Data Availability Statement: Not applicable.

Acknowledgments: The authors would like to thank: T. Mitina (Institute of Chemistry, R. Moldova) for AAS measurements; O. Petuhov (Institute of Chemistry, R. Moldova) for nitrogen sorption-desorption isotherms; M. Rusu (Institute of Chemistry, R. Moldova) for FTIR spectra; A. Puziy (Department of Chemistry and Chemical Technology, National Aviation University, Kyiv, Ukraine) for potentiometric titrations; and V. Vasilache (Department of Interdisciplinary Research—Science Field, A.I. Cuza University of Iasi, Romania) for SEM-EDX analysis.

Conflicts of Interest: The authors declare no conflict of interest.

References

1. Fergusson, J.E. The Heavy Elements: Chemistry. In *Environmental Impact and Health Effects*; Pergamon Press: Oxford, UK, 1990; pp. 211–212.
2. Tchounwou, P.B.; Yedjou, C.G.; Patlolla, A.K.; Sutton, D.J. Heavy metal toxicity and the environment. In *Molecular, Clinical and Environmental Toxicology*; Luch, A., Ed.; Springer: Berlin/Heidelberg, Germany, 2012; Volume 3, pp. 133–164. [\[CrossRef\]](#)
3. Meena, A.K.; Kadirvelu, K.; Mishra, G.K.; Rajagopal, C.; Nagar, P.N. Adsorption of Pb(II) and Cd(II) metal ions from aqueous solutions by mustard husk. *J. Hazard. Mater.* **2008**, *150*, 619–625. [\[CrossRef\]](#)
4. Coelho, G.F.; Goncalves, A.C., Jr.; Tarley, C.R.T.; Casarin, J.; Nacke, H.; Francziskowski, M.A. Removal of metal ions Cd (II), Pb (II), and Cr (III) from water by the cashew nut shell *Anacardium occidentale* L. *Ecol. Eng.* **2014**, *73*, 514–525. [\[CrossRef\]](#)
5. Järup, L. Hazards of heavy metal contamination. *Br. Med. Bull.* **2003**, *68*, 167–182. [\[CrossRef\]](#)
6. Jaishankar, M.; Tseten, T.; Anbalagan, N.; Mathew, B.B.; Beeregowda, K.N. Toxicity, mechanism and health effects of some heavy metals. *Interdiscip. Toxicol.* **2014**, *7*, 60–72. [\[CrossRef\]](#)
7. Lerebours, A.; Stentiford, G.D.; Lyons, B.P.; Bignell, J.P.; Derocles, S.A.P.; Rotchell, J.M. Genetic Alterations and Cancer Formation in a European Flatfish at Sites of Different Contaminant Burdens. *Environ. Sci. Technol.* **2014**, *48*, 10448–10455. [\[CrossRef\]](#) [\[PubMed\]](#)
8. Ward, J.F. DNA Damage Produced by Ionizing Radiation in Mammalian Cells: Identities, Mechanisms of Formation, and Reparability. *Prog. Nucleic Acid Res. Mol. Biol.* **1988**, *35*, 95–125. [\[CrossRef\]](#)
9. Santhosh, C.; Velmurugan, V.; Jacob, G.; Jeong, S.K.; Grace, A.N.; Bhatnagar, A. Role of nanomaterials in water treatment applications: A review. *Chem. Eng. J.* **2016**, *306*, 1116–1137. [\[CrossRef\]](#)
10. Mikhalovsky, S.; Voytko, O.; Demchenko, V.; Demchenko, P. Enterosorption in the treatment of heavy metal poisoning. *Chem. J. Mold.* **2021**, *16*, 9–27. [\[CrossRef\]](#)
11. Mishra, S.P. Adsorption-desorption of heavy metal ions. *Curr. Sci.* **2014**, *107*, 601–612.
12. Bisht, R.; Agarwal, M.; Singh, K. Heavy metal removal from wastewater using various adsorbents: A review. *J. Water Reuse Desalin.* **2016**, *7*, 387–419.
13. Lupascu, T. *Activated Carbons from Vegetal Raw Materials*; Stiinta: Chisinau, Moldova, 2004; 224p. (In Romanian)
14. Thouraya, B.; Abdelmottaleb, O. Improvement of oxygen-containing functional groups on olive stones activated carbon by ozone and nitric acid for heavy metals removal from aqueous phase. *Environ. Sci. Pollut. Res.* **2015**, *23*, 15852–15861. [\[CrossRef\]](#)
15. Wang, W.; Liu, Y.; Liu, X.; Deng, B.; Lu, S.; Zhang, Y.; Bi, B.; Ren, Z. Equilibrium adsorption study of the adsorptive removal of Cd²⁺ and Cr⁶⁺ using activated carbon. *Environ. Sci. Pollut. Res.* **2018**, *25*, 25538–25550. [\[CrossRef\]](#)
16. Duca, G.; Ciobanu, M.; Lupascu, T.; Povar, I. Adsorption of strontium ions from aqueous solutions on nut shells activated carbons. *Chem. J. Mold.* **2018**, *13*, 69–73. [\[CrossRef\]](#)
17. Ciobanu, M.; Lupascu, T.; Mitina, T.; Povar, I. Adsorption of Sr²⁺ ions from aqueous solutions on the activated carbon CAN-7 under dynamic conditions. In Proceedings of the Environment and Industry SIMI, Bucharest, Romania, 20–21 September 2018; pp. 23–30. [\[CrossRef\]](#)
18. Geetha, K.S.; Belagali, S.L. Removal of Heavy Metals and Dyes Using Low Cost Adsorbents from Aqueous Medium-, A Review. *IOSR J. Environ. Sci. Toxicol. Food Technol.* **2013**, *4*, 56–68; e-ISSN: 2319-2402, p-ISSN: 2319-2399.
19. Chakraborty, R.; Asthana, A.; Singh, A.K.; Bhawana, J.; Susan, A.B.H. Adsorption of heavy metal ions by various low-cost adsorbents: A review. *Int. J. Environ. Anal. Chem.* **2020**, *102*, 342–379. [\[CrossRef\]](#)
20. Rivera-Utrilla, J.; Sánchez-Polo, M.; Gómez-Serrano, V.; Álvarez, P.M.; Alvim-Ferraz, M.C.M.; Dias, J.M. Activated Carbon Modifications to Enhance Its Water Treatment Applications. An Overview. *J. Hazard. Mater.* **2011**, *187*, 1–23. [\[CrossRef\]](#)
21. Trikhleb, V.A.; Trikhleb, L.M. Method for Production of Carbon Cation Exchanger. Patent RU2105715 C1, 27 February 1998. (In Russian)
22. Nastas, R.; Ginsari, I.; Lupascu, T. Vegetal active carbons for adsorption of toxic metal ions. In Proceedings of the International Conference Achievements and Perspectives of Modern Chemistry, Chisinau, Moldova, 9–11 October 2019; p. 183, ISBN 978-9975-62-428-2.

23. Nastas, R. Specific Surface Properties of the Carbonaceous Adsorbents. Summary of the Ph.D. Thesis in Chemical Sciences. Ph.D. Thesis, Moldova State University, Chisinau, Moldova, 23 June 2006. (In Romanian)
24. Ginsari, I. Evaluation of the Influence of Carbonaceous Adsorbent Surface Chemistry on the Adsorption Process of Pollutants. Ph.D. Thesis, Moldova State University, Chisinau, Moldova, 17 September 2021. (In Romanian)
25. Ermolenko, I.N.; Liublner, I.P.; Guliko, N.V. *Element-Containing Carbons Fiber Materials*; Science and Technology: Minsk, Belarus, 1982; p. 272. (In Russian)
26. STAS 5388-80; Vegetal Activated Carbon. Testing Methods. Editura Tehnică: București, Romania, 1980; 18p. (In Romanian)
27. Boehm, H.P.; Diehl, E.; Heck, W.; Sappok, R. Surface oxides of carbon. *Angew. Chem. Int. Ed.* **1964**, *3*, 669–677. [[CrossRef](#)]
28. Boehm, H. Some aspects of the surface chemistry of carbon blacks and other carbons. *Carbon* **1995**, *5*, 759–769. [[CrossRef](#)]
29. Nastas, R.; Rusu, V.; Lupascu, T. Establishing the acid-base properties of activated carbons. *Stud. Univ. Mold.* **2016**, *96*, 170–177. (In Romanian)
30. Puziy, A.M.; Poddubnaya, O.I.; Gawdzik, B.; Sobiesiak, M.; Sprynskyy, M. Structural Evolution of Polyimide-Derived Carbon during Phosphoric Acid Activation. *C* **2022**, *8*, 47. [[CrossRef](#)]
31. Provencher, S.W. A Constrained Regularization Method for Inverting Data Represented by Linear Algebraic or Integral Equations. *Comput. Phys. Commun.* **1982**, *27*, 213–227. [[CrossRef](#)]
32. Provencher, S.W. CONTIN: A General Purpose Constrained Regularization Program for Inverting Noisy Linear Algebraic and Integral Equations. *Comput. Phys. Commun.* **1982**, *27*, 229–242. [[CrossRef](#)]
33. Puziy, A.M.; Matynia, T.; Gawdzik, B.; Poddubnaya, O.I. Use of CONTIN for Calculation of Adsorption Energy Distribution. *Langmuir* **1999**, *15*, 6016–6025. [[CrossRef](#)]
34. Puziy, A.M.; Poddubnaya, O.I.; Ritter, J.A.; Ebner, A.D.; Holland, C.E. Elucidation of the Ion Binding Mechanism in Heterogeneous Carbon-Composite Adsorbents. *Carbon* **2001**, *39*, 2313–2324. [[CrossRef](#)]
35. Gustafsson, J.P. Visual MINTEQ Ver.4.0 (4.04). 2023. Available online: <https://vminteq.com/> (accessed on 3 May 2023).
36. Tien, C.; Ramarao, B.V. On the significance and utility of the Lagergren model and the pseudo second-order model of batch adsorption. *Sep. Sci. Technol.* **2017**, *52*, 975–986. [[CrossRef](#)]
37. Ho, Y.S. Removal of metal ions from sodium arsenate solution using tree fern. *Process Saf. Environ. Prot.* **2003**, *81*, 352–356. [[CrossRef](#)]
38. Liu, Q.S.; Zheng, T.; Wang, P.; Jiang, J.P.; Li, N. Adsorption isotherm, kinetic and mechanism studies of some substituted phenols on activated carbon fibers. *Chem. Eng. J.* **2010**, *157*, 348–356. [[CrossRef](#)]
39. Largitte, L.; Pasquier, R. A review of the kinetics adsorption models and their application to the adsorption of lead by an activated carbon. *Chem. Eng. Res. Des.* **2016**, *109*, 495–504. [[CrossRef](#)]
40. Moreno-Castilla, C.; Ferro-Garcia, M.A.; Joly, J.P.; Bautista-Toledo, I.; Carrasco-Marin, F.; Rivera-Utrilla, J. Activated carbon surface modifications by nitric acid, hydrogen peroxide, and ammonium peroxydisulfate treatments. *Langmuir* **1995**, *11*, 4386–4392. [[CrossRef](#)]
41. Sheindorf, C.; Rebhun, M.; Sheintuch, M. A Freundlich-type multicomponent isotherm. *J. Colloid Surf. Sci.* **1981**, *79*, 136–142. [[CrossRef](#)]
42. Hutson, N.D.; Yang, R.T. Theoretical Basis for the Dubinin-Radushkevitch (D-R) Adsorption Isotherm Equation. *Adsorption* **1997**, *3*, 189–195. [[CrossRef](#)]
43. Johnson, R.D.; Arnold, F.H. The Temkin isotherm describes heterogeneous protein adsorption. *Biochim. Biophys. Acta* **1995**, *1247*, 293–297. [[CrossRef](#)] [[PubMed](#)]
44. Nastas, R.; Rusu, V.; Giurginca, M.; Meghea, A.; Lupascu, T. Alteration of Chemical Structure of the Active Vegetal Coals. *Rev. De Chim.* **2008**, *59*, 159–164. [[CrossRef](#)]
45. Akolekar, D.B.; Bhargava, S.K. Influence of thermal, hydrothermal, and acid-base treatments on structural stability and surface properties of macro- meso-, and microporous carbons. *J. Colloid Interface Sci.* **1999**, *216*, 309–319. [[CrossRef](#)] [[PubMed](#)]
46. Zawadzki, J. Infrared spectroscopy in surface chemistry of carbons. In *Chemistry and Physics of Carbon*; Thrower, P.A., Ed.; Marcel Dekker: New York, NY, USA, 1989; Volume 21, pp. 147–380.
47. Bingzheng, L. Characterization of pore structure and surface chemistry of activated carbons—A Review. In *Fourier Transform—Materials Analysis*; Salih, S., Ed.; InTech: Rijeka, Croatia, 2012; pp. 165–190.
48. Rodriguez-Reinoso, F.; Molina-Sabio, M. Textural and chemical characterization of microporous carbons. *Adv. Colloid Interface Sci.* **1998**, *76–77*, 271–294. [[CrossRef](#)]
49. Boehm, H.P. Surface oxides on carbon and their analysis: A critical assessment. *Carbon* **2002**, *40*, 145–149. [[CrossRef](#)]
50. Demirbas, E. Adsorption of Cobalt(II) Ions from Aqueous Solution onto Activated Carbon Prepared from Hazelnut Shells. *Adsorpt. Sci. Technol.* **2003**, *21*, 951–963. [[CrossRef](#)]
51. Zhang, X.; Hao, Y.; Wang, X.; Chen, Z. Adsorption of iron(III), cobalt(II), and nickel(II) on activated carbon derived from *Xanthoceras Sorbifolia* Bunge hull: Mechanisms, kinetics and influencing parameters. *Water Sci. Technol.* **2017**, *75*, 1849–1861. [[CrossRef](#)]
52. Prabakaran, R.; Arivoli, S. Removal of Cobalt (II) from Aqueous Solutions by Adsorption on Low cost activated carbon. *Int. J. Sci. Eng. Technol. Res.* **2013**, *2*, 271–283.
53. Vinod, K.G.; Ganjali, M.R.; Nayak, A.; Bhushan, B.; Agarwal, S. Enhanced heavy metals removal and recovery by mesoporous adsorbent prepared from waste rubber tire. *Chem. Eng. J.* **2012**, *197*, 330–342.

54. Vagheti, J.C.P.; Lima, E.C.; Royer, B.; Da Cunha, B.M.; Cardoso, N.F.; Brasil, J.L.; Dias, S.L.P. Pecan Nutshell as Biosorbent to Remove Cu(II), Mn(II) and Pb(II) from Aqueous Solutions. *J. Hazard. Mater* **2009**, *162*, 270–280. [[CrossRef](#)] [[PubMed](#)]
55. Lupascu, T.; Ciobanu, M.; Petuhov, O. Inflection points on the adsorption isotherms of strontium ion on oxidate activated carbons. In Proceedings of the International Conference Achievements and Perspectives of Modern Chemistry, Chisinau, Moldova, 9–11 October 2019; p. 81.
56. Yakout, S.M.; Elsherif, E. Batch kinetics, isotherm and thermodynamic studies of adsorption of strontium from aqueous solutions onto low cost rice-straw based carbons. *Carbon–Sci. Technol. Carbon–Sci. Technol.* **2010**, *1*, 144–153.
57. Shawabkeh, R.A.; Rockstraw, D.A.; Bhada, R.K. Copper and strontium adsorption by a novel carbon material manufactured from pecan shells. *Carbon* **2002**, *40*, 781–786. [[CrossRef](#)]
58. Arifi, A. Adsorption of Cesium, Thallium, Strontium and Cobalt Radionuclides Using Activated Carbon. *Asian J. Chem.* **2010**, *23*, 111–115.
59. Riddhish, B.R.; Bhavna, S.A. Sorption studies of heavy metal ions by salicylic acid–formaldehyde–catechol terpolymeric resin: Isotherm, kinetic and thermodynamics. *Arab. J. Chem.* **2015**, *8*, 414–426.
60. Ciobanu, M.; Botan, V.; Lupascu, T.; Mitina, T.; Rusu, M. Adsorption of strontium ions from water on modified activated carbons. *Chem. J. Moldova. Gen. Ind. Ecol. Chem.* **2016**, *11*, 26–33. [[CrossRef](#)]
61. Girgis, B.S.; Attia, A.A.; Fathy, N.A. Modification in adsorption characteristics of activated carbon produced by H₃PO₄ under flowing gases. *Colloids Surf. A Physicochem. Eng. Asp.* **2007**, *299*, 79–87. [[CrossRef](#)]
62. Mamba, B.B.; Nyembe, D.W.; Mulaba-Bafubiandi, A.F. Removal of copper and cobalt from aqueous solutions using natural clinoptilolite. *Water SA* **2012**, *35*, 307–314. [[CrossRef](#)]
63. Persson, I. Hydrated metal ions in aqueous solution: How regular are their structures? *Pure Appl. Chem.* **2010**, *82*, 1901–1917. [[CrossRef](#)]
64. Radovic, L.R. *Surfaces of Nanoparticles and Porous Materials*; Schwarz, J.A., Contescu, C.I., Eds.; Marcel Dekker: New York, NY, USA, 1999; 787p.
65. Osinska, M. Removal of lead(II), copper(II), cobalt(II) and nickel(II) ions from aqueous solutions using carbon gels. *J. Sol-Gel Sci. Technol.* **2017**, *81*, 678–692. [[CrossRef](#)]
66. Aggarwal, D.; Goyal, M. Adsorptive removal of cobalt from aqueous solution by activated carbons. *J. Ind. Pollut. Control.* **2005**, *21*, 347–360.
67. Gad, H.M.H.; Omar, H.A.; Aziz, M.; Hassan, M.R.; Khalil, M.H. Treatment of Rice Husk Ash to Improve Adsorption Capacity of Cobalt from Aqueous Solution. *Asian J. Chem.* **2016**, *28*, 385–394. [[CrossRef](#)]
68. Lupea, M.; Bulgariu, L.; Macoveanu, M. Adsorption of Cobalt(II) from aqueous solution using marine green algae—*Ulva lactuca* sp. *Bull. Polytech. Inst. Iasi* **2012**, *58*, 41–47.
69. Oliveira, R.C.; Hammer, P.; Guibal, E.; Taulemesse, J.M.; Garcia, J.R.O. Characterization of metal-biomass interactions in the lanthanum(III) biosorption on sargassum sp. using SEM/EDX, FTIR, and XPS: Preliminary studies. *Chem. Eng. J.* **2014**, *239*, 381–391. [[CrossRef](#)]
70. Atieh, M.A.; Bakather, O.Y.; Al-Tawbini, B.; Bukhari, A.A.; Abuilawi, F.A.; Fettouhi, M.B. Effect of Carboxylic Functional Group Functionalized on Carbon Nanotubes Surface on the Removal of Lead from Water. *Bioinorg. Chem. Appl.* **2011**, *2010*, 1–9. [[CrossRef](#)]
71. Radovic, L.R.; Morino-Castilla, C.; Rivera-Utrilla, J. *Chemistry and Physics of Carbon*; Radovic, L.R., Ed.; Marcel Dekker: New York, NY, USA, 2000; Volume 27, 227p.
72. Barton, S.S.; Evans, M.J.B.; Halliop, E.; Macdonald, J.A.F. Acidic and basic sites on the surface of porous carbon. *Carbon* **1997**, *35*, 1361–1366. [[CrossRef](#)]
73. Hasan, S.; Iasir, A.; Ghosh, T.; Sen, G.B.; Prelas, M. Characterization and Adsorption Behavior of Strontium from Aqueous Solutions onto Chitosan-Fuller’s Earth Beads. *Healthcare* **2019**, *7*, 52–70. [[CrossRef](#)]
74. Apak, R.; Atun, G.; Guclu, K.; Tutem, E. Sorptive removal of Cesium-137 and Strontium-90 from water by conventional sorbents. *J. Nucl. Sci. Technol.* **1996**, *33*, 396–402. [[CrossRef](#)]
75. Shahwan, T.; Erten, H.N. Characterization of Sr²⁺ uptake on natural minerals of kaolinite and magnesite using XRPD, SEM/EDS, XPS, and DRIFT. *Radiochim. Acta* **2005**, *93*, 225–232. [[CrossRef](#)]
76. Machida, M.; Amano, Y. Preparation and Modification of Activated Carbon Surface and Functions for Environments. In *The Handbook of Environmental Chemistry*; Springer Nature: Singapore, 2020; pp. 335–366.

Disclaimer/Publisher’s Note: The statements, opinions and data contained in all publications are solely those of the individual author(s) and contributor(s) and not of MDPI and/or the editor(s). MDPI and/or the editor(s) disclaim responsibility for any injury to people or property resulting from any ideas, methods, instructions or products referred to in the content.